Joana Lourenço Tavares

Bachelor in Micro and Nanotechnologies Engineering

Fabrication of Highly Reflective Bottom Electrodes for Inverted Top-emission OLED Applications

Dissertation submitted in partial fulfillment
of the requirements for the degree of

Master of Science in
Micro and Nanotechnologies Engineering

Adviser: Prof. Dra. Elvira Fortunato, Full Professor,
Faculty of Sciences and Technology,
NOVA University of Lisbon
Co-Adviser: Dr. Tung Huei Ke, Senior Researcher,imec

FACULDADE DE CIÊNCIAS E TECNOLOGIA
UNIVERSIDADE NOVA DE LISBOA

September, 2018

Fabrication of Highly Reflective Bottom Electrodes for Inverted Top-emission OLED Applications

“Scientists dream about doing great things, Engineers do them” – James A. Michener

Acknowledgements

I would like to demonstrate how thankful I am to everyone involved in these last amazing 5 years that culminated with a master degree in Micro and Nanotechnologies Engineering.

Firstly, I would like to thank my professor and advisor Prof. Elvira Fortunato for the opportunity to have myfirst professional experience in a vibrant, advanced and high tech company as imec and to Prof. Paul Heremans for accepting to receive me in his wonderful team.

Secondly, I want to recognise Tung Huei as an excellent mentor who never let me lose the focus and who always believed in my capabilities. I will always be grateful to you and proud to have made you proud.

Next, thank you Dieter Vander Velpen who had an enormous contribution for this thesis. I will never forget our first substrate cleaning. Thank you Dieter for more than a big friend being an excellent teacher and partner. I am already missing our lab laughs and cleanroom talks. You know how big you are, how far you will arrive and how much I like you.

A very special thank to Takashi Goto, from Fujifilm. Although your name is not in the first page you were a pillar in this thesis. I want particularly mention you as an incredible human being, full of knowledge to share with everyone.

I want to show my deepest gratitude to all the LAE group from imec that made memorable those 6 months. You guys are an incredible team. All of you have contributed, in some way, to my success both personally and professionally and I will never forget it. Particularly, Myriam Willegems, Manoj Nag and Erwin Vandenplas deserve my recognition for their patience and for their contribution with knowledge, challenges and ideas to the improvement of this thesis.

I would also like to thank my professors, since the basic school until university, who offered me all the tools to build my future and my professional career. Particularly, Prof. João Ferereira, Prof. Maria José Castro, Prof. Luís Pereira, Prof. Hugo Águas and Prof. Rui Igreja, thank you for your great work.

Thank you to all my Portuguese friends, for the unconditional presence in my life. To Ana Rita Gomes for being the best sister from another mister. To Carolina Leitão and Mafalda Caldas, who could not have been better partners, better friends and better family along this 5 years. FCT is done, Leuven is done, but the world is waiting for us. To all the others, I know that no matter where and how life takes us, I can always count on you.

My friends from Leuven, Vladimir, Guillaume, Prakar, Ravi, Gema, Hany, Tzu Yi, Madji, Sheri and Subhobroto, you filled my heart with love and friendship and I am waiting for all of you in Portugal.

A singular appointment to you, Andrej, who were the best housemate ever. You are the best person who I could have asked to be part of my life.

Last, but not least, thanks to my lovely family, without them I could not be here. Thanks for all the support and for the opportunity to have an education for the future. To my mother, Aurora, and my father, Joaquim, for giving me wings to fly, for giving me an amazing education and for having always dried my tears and joined me in my laughs. To my brother, who is the best friend and the best example in my life. Thank you João for always letting me be your shadow, I have learnt so much with you. And to my two stars, my guardian angels, who always protect me.

Abstract

The demand for more air-stable and high resolution devices are opening the space for inverted top-emission OLEDs in the displays market. To realize these high-performance devices, a combination of a highly reflective bottom electrode with an efficient electron injection layer is essential to achieve high luminance efficiency and low driving voltage, respectively.

The aim of this thesis was to develop a new highly reflective stack and a corresponding method for high resolution patterning to enable future top-emission iOLED applications. First, the deposition methods for a multilayer reflective stack were developed. Initially, a structure using silver as reflective thin film and ITZO as electron injection layer was used. Reflective and transmission measurements together with optical simulation were executed to optimize the thickness of each sputtered thin film in the final stack. During the development, the oxidation of Ag prevented the high reflectivity of the layer. To mitigate this issue, a new stack with an ITO interlayer between Ag and ITZO layers was created to prevent silver oxidation from the ITZO deposition process. Finally, optimized samples with a configuration of Ag(50 nm)/ITO(5 nm)/ITZO(80 nm) were demonstrated with a reflectivity > 78% in the visible range.

To obtain high resolution feature sizes on the developed stack, the photolithography recipe to pattern the multilayer stacks with resolution down to 5um was also developed. During this project, different liquid etchants were tested to pattern the structure in two wet-etching steps. The quality of the etch were analysed by atomic force microscope and optical microscope images. Images of individual ITZO layers demonstrated the importance of using Ti Prime before photoresist spin-coating to improve the quality of the etch. At the end, cross-sections of the full stack showed that well-defined hills and valleys were achieved when samples were dipped in 10% mixed acid etchant for 30sec at RT followed by a dip in 75% PWES solution for 5 sec at 45°C.

Key-words: Inverted top-emission OLEDs, reflective cathode, electron injection, sputtering, photolithography, wet etching

Resumo

A necessidade de dispositivos mais estáveis ao ar e com maiores resoluções está a abrir caminho para os *inverted top-emission* OLEDs no mercado dos mostradores. Para produzir esses dispositivos de elevado desempenho, é necessária uma combinação entre um elétrodo extremamente refletivo e uma eficiente camada injetora de eletrões para alcançar elevada eficiência de luminância e baixa corrente de condução, respetivamente.

O objetivo desta tese era desenvolver uma estrutura nova e extremamente refletora e o correspondente método de padronização com elevada resolução para futuras aplicações em *inverted top-emission* OLEDs. Primeiramente, foi desenvolvido o método de deposição para uma estrutura refletora de multicamadas. Isto começou com uma estrutura que usava prata como filme refletor e ITZO como camada injetora de eletrões. A otimização da espessura de cada filme depositado por pulverização catódica foi feita através de medições de reflexão e transmissão juntamente com simulação ótica. Durante a otimização, foi descoberto que a oxidação da prata reduzia a refletividade da estrutura final. Para solucionar esse problema e prevenir a oxidação da prata durante o processo de deposição do ITZO, foi inventada uma nova estrutura com uma camada de ITO entre as camadas de Ag e ITZO. Finalmente, as amostras otimizadas com configuração de Ag(50 nm)/ITO(5 nm)/ITZO(80 nm) mostraram refletividade > 78% na região visível do espetro.

Para obter estruturas padronizadas de elevada resolução, foi também desenvolvida a receita do processo de fotolitografia. Durante este projeto, diferentes soluções foram testadas como agentes erosivos para padronizar essa estrutura em dois passos de erosão húmida. A qualidade da erosão foi analisada através de imagens de AFM e microscópio ótico. Imagens de filmes de ITZO demonstraram a importância de usar *Ti Prime* antes do fotoresiste para melhorar a qualidade a erosão. Por fim, imagens da estrutura completa mostraram que é possível obter vales bem definidos quando as amostras foram imersas em 10% *mixed acid etchant* por 30 seg a temperatura ambiente, seguidas de imersão em 75% *PWES* por 5 seg a 45°C.

Palavras-chave: *Inverted top-emission* OLEDs, cátodo reflector, injecção de eletrões, pulverização catódica, fotolitografia, erosão húmida

Contents

List of Figures

List of Tables

Acronyms

AFM – Atomic Force Microscope
DC – Direct Current
EBL – Electron Blocking Layer
EIL – Electron Injection Layer
EML – Emissive Layer
ETL – Electron Transport Layer
HBL – Hole Blocking Layer
HIL – Hole Injection Layer
HOMO – Highest Occupied Molecular Orbital
HTL – Hole Transport Layer
HyLEDS – Hybrid Light Emitting Devices
IGZO – Indium Gallium Zinc Oxide
iOLEDS – Inverted Organic Light Emitting Devices
IPA – Isopropanol
IR – Infrared
ITO – Indium Tin Oxide
ITZO – Indium Tin Zinc Oxide
LCD – Liquid Crystal Displays
LUMO – Lowest Unoccupied Molecular Orbital
OLEDS - Organic Light Emitting Devices
OM – Optical Microscope
PLD – Pulse Laser Deposition
ppi – pixel per inch
PVD – Physical Vapor Deposition
PWES – Phosphoric Acid Etching Mixture
RGB – Red, Green and Blue
RT – Room Temperature
SCCM – Standard Cubic centimetres per Minute
TAOS – Transparent Amorphous Oxide Semiconductor
TFT – Thin Film Transistors
TOLEDs – Transparent Organic Light Emitting Devices
TVs – Televisions
UV – Ultra-Violet
VR – Virtual Reality
WF – Work Function

Symbols

n – Refractive Index

k – Extinction Coefficient

E_g – Energy Gap

Motivation and objective

Even though the OLEDs have already begun to be investigated since 1987 by Chong W.Tang and Steven Van Slyke at Eastman Kodak [1], their competitiveness with the liquid crystal display (LCD) technology in the displays market only took place decades later with their first application in displays by Kodak in 2003 [2].

OLED's properties such as light weight, small thickness, high contrast ratios, low operation voltage, fast switching, wide viewing angle, fast response time, and high luminance combined with the possibility of processing on flexible, transparent and large substrates make OLEDs a suitable technology for todays' requirements [3]. However, the performance of this device is strongly limited by the low environmental stability of the organic materials, requiring a rigorous encapsulation to limit the degradation effects. This directly affects the final cost and effectiveness of OLEDs [4]. The development of top emitting devices with an inverted structure (bottom cathode) has been studied as a solution not only to build encapsulation-free OLEDs but also to increase the aperture ratio of the pixel [5],[6]. The absence of an appropriate electron injection layer (EIL) is still an obstacle to the realization of inverted OLEDs. Since a large energy barrier for electron injection exists between the cathode and the organic layer, materials capable to lower that barrier are needed. Metal oxides, in particular, transparent amorphous oxide semiconductors (TAOS), are considered to address this issue hence their application as an EIL has been studied [7].

At the same time, high resolution applications (Figure 1.1 (a)) demand a cost-effective manufacturing technology. Photolithography promises to provide a fabrication route for OLED patterning with submicron feature sizes, large-area production and compatibility with existing FAB tools for the creation of different product classes (Figure 1.1 (b)) [8],[9].

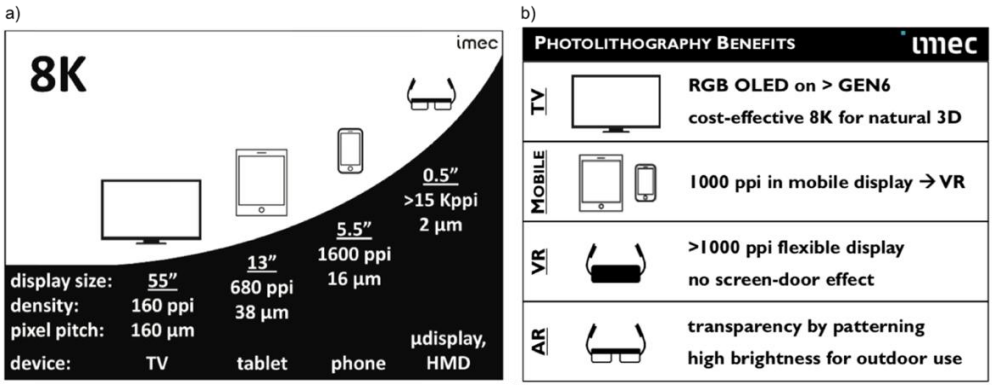

Figure 1.1 – a) Pixel density and pitch necessary to reach 8K resolution for different display types (television, tablet, smartphone and microdisplay/head-mounted display), adopted from [8]*. b) OLED photolithography benefits for different product classes with unique and specific requirements, adopted from* [9].

In this project, a highly reflective bottom electrode stack was developed to increase the performance of an inverted top-emitting OLED. The electrode stack comprises of silver as a highly reflective bottom electrode and indium tin zin oxide (ITZO), a TAOS, as EIL and optical spacer to achieve the ideal thickness that increase the light outcoupling coefficient of the final device. Photolithography patterning was employed as the production technique to achieve individual pixels for high resolution display application.

1 Introduction

This chapter describes why inverted top-emission OLEDs can be a promising technology for future displays application. Furthermore, it justifies the importance of patterning and developing a highly reflective stack made by silver and indium tin zinc oxide.

1.1 Displays importance: OLEDs technology

Nowadays, we are in an era of overflowing visual information, which makes the displays industry one of the most innovative industries. Display applications, such as TVs, smartphones, laptops and, more recently, virtual reality and augmented reality seem to have one common demand: resolutions above HD (high definition) and towards 4K and 8K to obtain better image depth and to create the perception of three-dimensional scene in a flat panel. Consequently, the need for introducing new technologies and for reducing cost of manufacturing has been impressive and does not seem to slow down. Among the different flat panel displays technologies, OLED displays became more and more important in recent years [8].

Organic light emitting devices (OLEDs) with a bi-layer structure were firstly reported by Ching W.Tang and Steven Van Slyke at Eastman Kodak in 1987 [1]. From there, their commercialization has grown in the full-color display industry due to their intrinsic characteristics and wide range of applications. Although small high-resolution OLED displays are widely used for smartphones/tablets, and large OLED televisions are being commercialized, numerous issues still remain, such as lifetime, image sticking, power consumption, and production cost [10]. One of the weaknesses of these devices is that most of the organic materials used to build an OLED are highly sensitive to oxygen, moisture, solvents, temperature and radiation, leading to the degradation of the displays. Encapsulation methods, new material approaches, different architectures and new patterned processes have been intensely studied and extensive research efforts have been done to increase not only the efficiency and color stability but also the lifetime and resolution of these devices [11],[12].

1.2 Highly reflective electrode for OLED application

OLED is an electronic device made by organic thin film layers sandwiched between two conductive electrodes as demonstrated in Figure 1.1. All the layers have an important and well-defined role in the final device: the anode is used to inject holes into the organic layers and the cathode is used to inject electrons into the organic layers. To match the work function (WF) of both electrodes with the energy levels of the organic layers (HOMO and LUMO), enhancing the efficiency of charge injection, a hole injection layer (HIL) and an electron injection layer (EIL) are introduced between their respective electrode and transport layer. Electrons and holes have different mobilities in different layers, hence to create a proper OLED, these layers are also employed to slow down the carriers with the highest mobility, electrons, and to inject and transport into the emissive layer the ones with the lowest mobility, holes, as fast as possible. The roll of the hole transport layer (HTL) and the electron transport layer (ETL) is to move carriers to the emissive layer as well as block oppositely charged carriers from entering this layer confining the carriers in the emissive layer, thus increasing the chance for recombination. A hole blocking layer (HBL) and electron blocking layer (EBL) can also be inserted after the respective

ETL and HTL to constrain the carriers in the recombination zone, raising the number of produced photons. An EBL should have good transport properties for holes and a LUMO level higher than the LUMO level of the emissive layer to confine the electrons inside the emissive layer (EML). On the other hand, HBL should transport electrons efficiently and have a HOMO level lower than the HOMO level of the EML. All the layers are deposited on a substrate that can be glass, plastic or metal foil depending on the application [13].

When a bias is applied to this structure, an electric field appears and holes and electrons are injected from the respective electrodes to the EML where part of them recombine and emit light.

OLED architectures can be distinguished by the emission direction. Hence, depending on where the light escapes the final structure, an OLED can be bottom or top emitting as presented in scheme (a) and (b) of Figure 1.1.

In bottom-emitting devices, the light travels through the layers and leave the device from the transparent substrate. It requires a transparent and conductive anode to transmit the light and a reflective electrode, cathode, on top of the organic layers to reflect the light. As the transparent bottom electrode is deposited prior to the organic layers, there are no special restrictions concerning the material to be used [11]. The main issue of this approach comes from the fact that OLED is a current driven device, so at least two transistors are needed to drive each pixel. Since, the TFT array is manufactured on the transparent substrate before OLED materials deposition, the opaque TFT blocks a significant portion of the transmitted light. Thus, if the device employs the conventional bottom-emitting design, the aperture ratio of active matrix OLED is diminished, affecting the achievable resolution limits, and the current loading of the OLED increases, reducing the lifetime [14], [15].

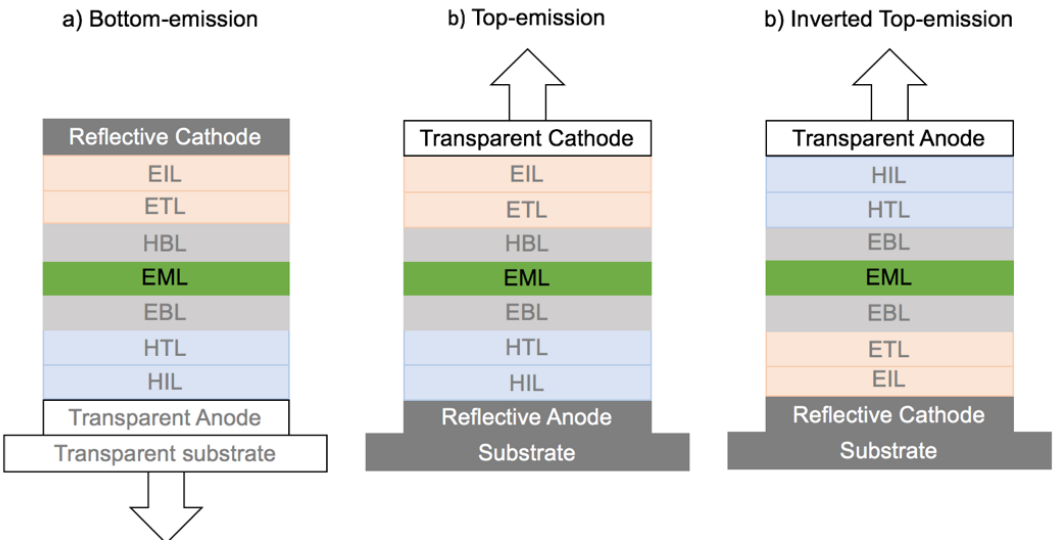

Figure 1.1 - Comparison of bottom (a), top (b) and inverted top (c) stacked device architecture. Adapted from [12].

1.2.1 Why top emission OLED?

Top-emitting structures, where the light is emitted away from the carrier substrate and the backplane pixel circuit, can be built on different types of opaque substrates, including metal foils and flexible materials. Hence, the TFT array necessary to drive the OLED can be hidden below the organic emitting layers solving the problem of reduced aperture ratio. However, a transparent electrode has to

be deposited on top of the organic stack, which considerably reduces the choice of appropriate materials, often limited to metal films with only moderate transmittance. Also the deposition technique of this layer requires special attention, since techniques which introduce damage to the organic layers cannot be applied [14]. In this configuration, also a high reflective bottom electrode is necessary. As a consequence of having two highly reflective contacts, top-emitting OLEDs (TOLEDs) usually exhibit strong microcavity effects like spectral narrowing and a strong blue shift of the emission with increasing viewing angle, leading to poor color quality and lower efficiencies [11]. To compensate these undesirable effects and reach a comparable performance with bottom-emission devices, many progresses of top-emitting OLED performance and outcoupling have been reported. Different metal structures and materials have been used to achieve better reflectivity and charge injection properties and an organic capping layer has been introduced to improve light extraction [16].

1.2.2 Lifetime issue: EIL and ETL are more sensitive to air conditions

Another great challenge in conventional OLEDs is related with the intrinsic low environmental stability of the organic materials, which are extremely sensitive to moisture and oxygen. For example aluminium, a common material used as cathode, has a low work function making it extremely susceptible to oxidation when exposed to air. Also, most electron injection materials suffer from the same problem. Considering both air-sensitive cathode and electron injection layer, the final device must be rigorously encapsulated to ensure good device stability and lifetime. This solution directly affects the final cost of the OLED, reducing the competitiveness of this technology [7].

1.2.3 Inverted OLED: better lifetime, but higher driving voltage

A top-emitting structure based on inverted organic layers (anode as top electrode), as represented in scheme (c) of Figure 1.1, was demonstrated by Dobbertin et al in 2003 [17] and not only simplifies the encapsulation of glass-based OLEDs but also allows for flexible/stretchable OLEDs. Furthermore, the electron injection layer of an inverted OLED (iOLED) is deposited before the organic layers not to damage them and increases the range of suitable materials and the lifetime of the final device. Nevertheless, reported inverted devices have higher driving voltage compared to non-inverted structures, as a result of a poor electron injection from the bottom cathode due to the sharp cathode-ETL interface. To match the work function of the bottom electrode with the energy levels of the organic layer (HOMO and LUMO) the energy barrier should be decreased and the efficiency of charge injection enhanced, hence efficient and air-stable electron injections layers have been intensely studied [7],[10],[18],[19]. An efficient EIL has the following requires [10]:

1. Low work function for a low electron injection barrier with an EML
2. High electron mobility is not needed because a very thin EIL layer would be sufficient.
3. Chemically stable and preferably comprised of only abundant nontoxic elements that enable a low production cost.

1.2.4 Transparent Amorphous Oxide Semiconductor as EIL in inverted OLEDs

The research in TAOS goes back to 1996 when Hosono et al. proposed the portion of the periodic table, highlighted in Figure 1.2, as the candidate elements to fill the need of materials with the dual merits of transparent conductors and amorphous materials [20]. Hosono revealed that metal oxides

composed of heavy metal cations with an electronic configuration $(n-1)d^{10}ns^0$, where $n \geq 4$, can meet the requirements for wide-gap amorphous oxides with high electron mobilities (~10 $cm^2V^{-1}s^{-1}$) [20].

He also discovered that the strong tendency of simple binary oxides such as of ZnO, SnO_2, and In_2O_3 to crystallize can be avoided by combining with cations in a multicomponent system to confuse the lattice as to which structure type to adopt, thereby frustrating crystallization and forming amorphous structures [21].

11	12	13	14	15	
29 Cu 63.54	30 Zn 65.37	31 Ga 69.72	32 Ge 72.59	33 As 74.92	4
47 Ag 107.87	48 Cd 112.40	49 In 114.82	50 Sn 118.69	51 Sb 121.75	5
79 Au 196.97	80 Hg 200.59	81 Tl 204.37	82 Pb 207.19	83 Bi 208.98	6

Figure 1.2 - The portion of the periodic table for selecting amorphous oxide semiconductor cations. Adopted from [21].

From that work, TAOS impressively immerged in the TFT industry owing to their unique properties such as high work function, high transparency in visible range, good electrical conductivity, tunable morphology, chemical stability, low temperature processing, good uniformity and the possibility of deposition on large areas with low-cost and mature techniques [22]. In 2004, the first TAOS TFT using an amorphous In–Ga–Zn–O (a-IGZO) channel deposited by pulsed laser deposition (PLD) was presented [23].

Nowadays, oxide TFTs which use TAOS materials as a channel layer are expected to be useful to drive large-sized OLEDs not only due to scalability, homogeneity and production cost but also because they can provide the mobility necessary to achieve high-quality moving images on displays [6].

However, certain technical issues still remain to be overcome for practical applications, like higher stability and compatibility with the OLED structure [6]. As explained by Hosono in a conference about transparent amorphous oxide semiconductors: “currently applied small OLEDs are driven by p-channel low temperature polysilicon (LTPS) TFT using normal stacking structure (cathode top). Since oxide TFTs only work as n-channel, the device stacking sequence are required to be reverse (...)” [6]. Although, as discussed in section 1.2.3 realizing inverted OLEDs with similar performance to conventional OLED structures is still a challenge caused by the lack of appropriate electron-injection and transport materials.

In 2011, M. Sessolo et al. reported a solution to surpass the challenge that has been investigated since 2006 [5]: “Metal oxides could be used as efficient electron injection contacts in inverted OLEDs. These hybrid organic-inorganic light emitting diodes (HyLEDs) use relatively thick semiconducting metal oxide layers that facilitate injection of electrons in the organic layers. As they are more robust to environmental influences, they should provide better stability for the whole organic device.”

In this project, ITZO, a n-type semiconductor, was deposited and patterned to be used as EIL and optical spacer in inverted top emitting OLEDs. ITZO is a hopeful TAOS to be used as TFT channel layer to drive large-sized and high resolution OLED displays as it has achieved a higher mobility (~31.4 $cm^2V^{-1}s^{-1}$) than IGZO. An inverted and flexible device using this material not only as channel layer in the TFTs, but also as EIL layer, has already been presented. As seen in Figure 1.3, the luminance-voltage characteristic of this device achieve higher efficiency and lower driving voltage than a conventional ZnO-based iOLED [24].

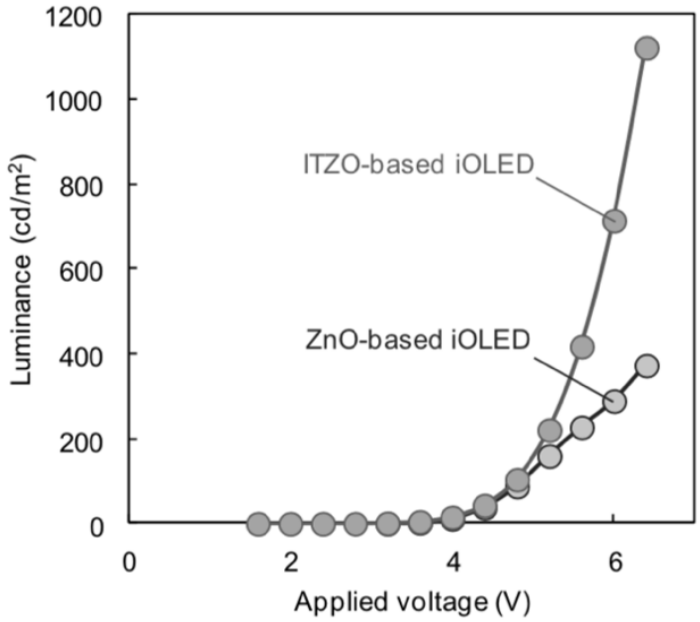

Figure 1.3 - Luminance-voltage characteristic of ITZO-based and ZnO-based iOLEDs, adopted from [24] *.*

1.2.5 ITZO as optical spacer

Efficiencies in OLEDs can be optimized by tuning the thickness of certain layers, creating an optical space to maximum the out-coupling efficiency. Thus, an optical spacer that is transparent in the visible range is required. Unfortunately, most of the organic electron transporting materials shows lower mobility compared to the hole transport materials. So, it is preferred to reduce the layer thickness of organic EIL for better device efficiency. Otherwise, increasing organic EIL thickness will result in higher driving voltage. On the other hand, ITZO shows much higher mobility compared to organic EIL. At the same time, its transparency to the visible light allows thinner or ticker layers without comprising the device out coupling. So, it is interesting to explore its application as optical spacer for OLED applications [25].

1.3 Photolithography as Patterning Process

With the eyes on iOLEDs application, this master thesis focused on the development of a reflective bottom electrode fabricated through a photolithography process. This is a standard process flow for backplane fabrication in display industry. In the manufacture of the devices, etching is an essential process in photolithography. Wet etching is a cheap and simple but hard to control and to reproduce process [26]. In this thesis, due to high selectivity, fast etch rate and the facility to implement, liquid

etchants were used to remove the materials from the exposed areas. Finally, the etching recipe for the developed multilayer stack was optimized to achieve high resolution electrodes for OLED applications.

2 Materials and Methods

This chapter explains the experimental conditions and techniques used during this project. It starts with the optical simulation study, followed by how the samples were produced and how they were analyzed.

2.1 Optical Simulation

At first, an optimization of thickness was performed using an optical model to find the OLED final structure with the highest efficiency. The ideal point was determined taking into account the complex index of refraction (n+jk), where n is the refractive index, k is the extinction coefficient, linked to the absorption coefficient, of each material that light finds during its path through the full stack. The model combines this complex index with the thickness of the layers and graphically shows the condition with the highest relative light outcoupling coefficient. In this thesis, to optimize the thickness of ITZO and ITO, a simulation considering the inverted top-emission stack already used by OLED group from LAE at imec were carried out. Nevertheless, silver was introduced as bottom contact, ITO as protective layer and ITZO as EIL.

2.1.1 Optical constant measurement - ellipsometry

The complex index of refraction (n+jk) of each material used in the optical simulation was determined using a multi-angle analysis by a spectroscopic ellipsometer sopra tool and the results are accessible in Appendix A . After the measurement, the data was fed into an optical model that takes into account the physical properties of the each film, producing a readout of not only the nk value, but also the thickness of the film.

2.2 Sample Production

2.2.1 Substrate Cleaning

All the 30 mm $\times$ 30 mm glass substrates were cleaned inside an ultrasonic bath at 55°C for at least 5 minutes in six consecutive steps: a soap bath, a deionized water bath, two consecutive acetone baths and two consecutive isopropanol (IPA) baths. After that, the samples were placed in UV-ozone environment for 15 minutes.

2.2.2 Thin Film Deposition - Sputtering Deposition

In this project, DC magnetron sputtering, a physical vapor deposition (PVD), was employed as the deposition method for all the layers due to its inherent advantages for producing uniform coatings over large areas with high reproducibility. All the depositions were sequentially done at room temperature without intentional target heating and a final structure with a configuration of Glass/Silver/ITO/ITZO was achieved. The thickness of each film was adjusted during the process according to the optical simulation and the etch rate.

Each sample production started with a silver thin film deposition on top of cleaned glass substrates using a tool named Lab 18 from Kurt J. Lesker company. An Ag alloy target was bombarded with pure argon (Ar) atoms with a deposition rate of 0.64 nm/sec.

Thereafter, an ITO and ITZO layer was deposited in Nimbus 310 NEEX system. Table 2.1 indicates the experimental conditions for both deposition. These deposition conditions have already been optimized by TFT group at imec.

Table 2.1- Conditions of sputtering ITO and ITZO thin films.

	TARGET COMPOSITION (WT.%)	DC POWER (W)	AR FLOW (SCCM)	O_2 FLOW (SCCM)	SPEED (MM/SEC)
ITO	In(90%)/Sn(10%)	1000	200	6	36.1
ITZO	In(44%)/Sn(12%)/Zn(44%)/Al(1%)	1000	100	30	40.6

2.2.3 Patterning Process - Photolithography

After deposition of the bottom electrode, protective layer and EIL, photolithography was used to define the openings of the uniform layers. The surface was coated with Ti prime followed by IX845 photoresist. Immediately after spin-coating at 4000 rpm for 30 sec, each previous layer was individually baked at 120 °C for 1 min. Then, the photoresist was exposed to UV light using a photolithography mask, plafet 5.0, during 2.4 sec in Karl Suss MA6 mask aligner. Afterwards, the photoresist was developed inside an OPD 5262 bath for 80 sec at RT. The uncovered stack was finally removed by wet etching process. The remained photoresist was detached with microstrip 2001 solution for 10 min at RT.

2.2.3.1 WET etching

In this thesis, an optimization of wet etching was performed. To remove the three materials from the non-protectives zones, oxalic acid, PWES and mixed acid etchant solutions were tested for different times until well defined vertical profiles were achieved.

2.3 Sample Characterization

2.3.1 Reflection and Transmission measurements

Since the aim was achieving a highly reflective bottom electrode, reflection and transmission measurements at near normal incidence in visible light range, 330 nm to 850 nm, using a silicon detector were done for each deposited film using a spectral response equipment.

2.3.2 Optical Microscope (OM)

The results of the photolithography patterning process, particularly the effect of distinct etchants under different conditions in the obtained structures, were observed through an optical microscope, Olympus AX70. This image technique was particularly useful to evaluate the etching process between each layer etching.

2.3.3 Atomic Force Microscope (AFM)

The topography of each sample after the etching process was investigated via the tapping mode of an atomic force microscope: Bruker Dimension Edge. The influence of different etchant rates in the profile of the structures as well as the importance of a Ti prime layer before the photoresist was understood when the AFM data was visualized and analyzed using Gwyddion software.

3 Results and Discussion

In this chapter, all the obtained results will be presented and discussed. It starts, in section 3.1, with an overview about the project. Then, section 3.2 shows the effort to optimize the bottom electrode stack in terms of optical characterization. Finally, the photolithography process using wet-etching to pattern the full developed stack is described in section 3.3.

3.1 Stack design strategy overview

As mentioned before, the aim of this work was to develop and fabricate a high resolution and highly reflective bottom electrode for inverted top-emission OLEDs. To obtain a high efficiency OLED, a highly reflective electrode with an effective injection layer are needed. Thus, a layer of ITZO on top of an Ag film was the first approach in this project.

However, after a spectral response characterization, it was found impossible to use this structure because silver oxidizes immediately during ITZO deposition, thus losing its inherent high reflection as will be discussed in section 3.2.3.

Silver oxidation was prevented using an ITO interlayer. ITO is widely used as an electrode in OLED technology and it has already been deposited on top of silver in many other research works [27], [28]. Also the transparent properties and process compatibility make this material suitable as a protective layer. After optical simulation tests and reflection measurements, presented in section 3.2.4, a multilayer Ag(100 nm)/ITO(90 nm)/ITZO(30 nm) structure was deposited and a photolithography process was initiated. During the etch procedure, ITO revealed a much lower etch rate than ITZO using 5% oxalic acid solutions as etchant. As wet etching is an isotropic process, the etch could end without any ITZO on top of ITO. To overcome this issue, an ITZO layer ticker than ITO and a new etchant were optimized and implemented. Section 3.3.5 shows that it was possible to successfully etch a structure with Ag(50 nm)/ITO(5 nm)/ITZO(80 nm).

Figure 3.1 schematizes the three phases of this project.

Figure 3.1 - Stack strategy during the process flow.

3.2 Reflective Electrode Stack Optimization

3.2.1 Silver deposition

In top-emitting OLEDs, high reflectivity of the bottom electrode is crucial to achieve a device with high luminance efficiency. Among various metals, Ag has the highest reflectivity for visible light [29]. As shown in Figure 3.2, the reflection increases by increasing silver film thickness from 50 nm to 100 nm. Both films were deposited under the same experimental conditions whereby it is possible to conclude that the difference in reflection is only related with the thickness. The lower reflectivity of Ag with 50 nm could be caused by many different reasons: the film density, oxidation in air, scattering due to different grain size, etc [30].

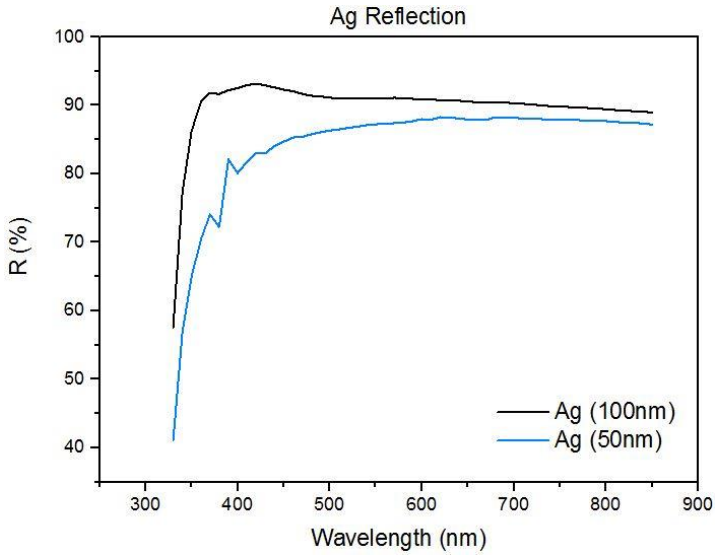

Figure 3.2 -Spectral characteristic of 100 and 50 nm of Silver.

3.2.2 ITZO deposition

The primary requirement for a TAOS to be used as EIL in top-emitting devices is the transparency to the visible light, consequently the effect of the oxygen partial pressure on the optical properties of IZTO films were examined. As demonstrated in literature [31], an ITZO thin film deposited under 30sccm of O_2 allows higher mobility than a film deposited with lower oxygen content. Thus, a comparison between the transmissions of films deposited under different oxygen contents were done.

The results of Figure 3.3 demonstrate that a sputtering process with 30 sccm of oxygen inside the chamber lightly improved the transmittance of the ITZO film. This may confirm the theory that an adequate amount of oxygen during the deposition leads to the reduction of the doped metallic Sn and Zn oxide complexes in the IZTO film, increasing its transmittance [28]. It is already known that the introduction of oxygen in the chamber contributes to carrier generation such as oxygen vacancies [29].

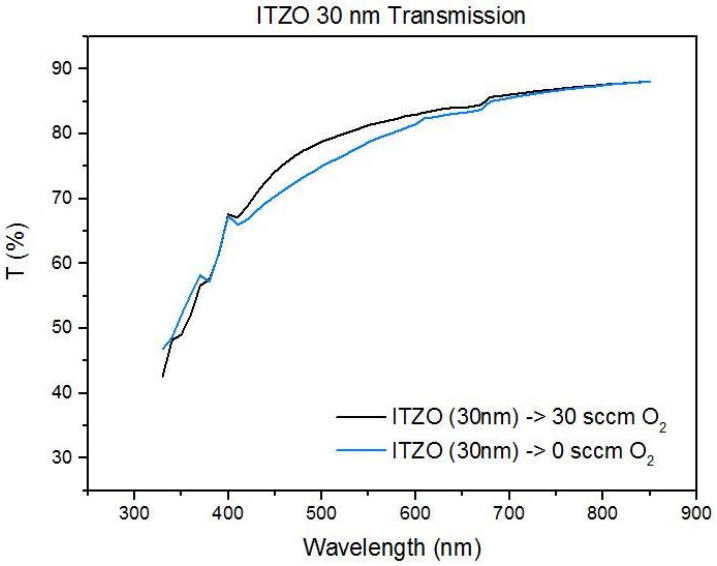

Figure 3.3 – Variation of optical transmission of ITZO films grown under different oxygen contents.

3.2.3 Silver/ITZO deposition

To enhance the carrier injection in the final device, decreasing the mismatch between the work function of silver and the HOMO of the organic material, a reflective stack with a configuration of Ag(100 nm)/ITZO(30 nm) was deposited sequentially onto glass substrates followed by a spectral response characterization. Figure 3.4 demonstrates that when an ITZO layer was deposited on top of a sputtered silver film, the reflectivity of this multilayer stack was lower than the reflectivity of a single silver layer rather oxygen was introduced during the deposition or not. It could be due to silver oxidation by the following general reaction [34]:

$$4\,Ag + O_2 \longrightarrow 2\,AgO$$

In fact, silver metal can be oxidized in an O_2/Ar atmospheric flow leading to different crystalline phases depending on the deposition time and consequently the thickness of the film. X-ray diffraction and field emission scanning electron microscope could be used to characterize these phases and to investigate the morphological microstructures, respectively [35]. Even without adding oxygen to the deposition, silver oxidation could be the explanation for the lower reflectivity once it is not possible to know how much oxygen was released from the target to the substrate during the sputtering process. Thus, it was necessary to study a method to reduce the Ag oxidation during ITZO deposition.

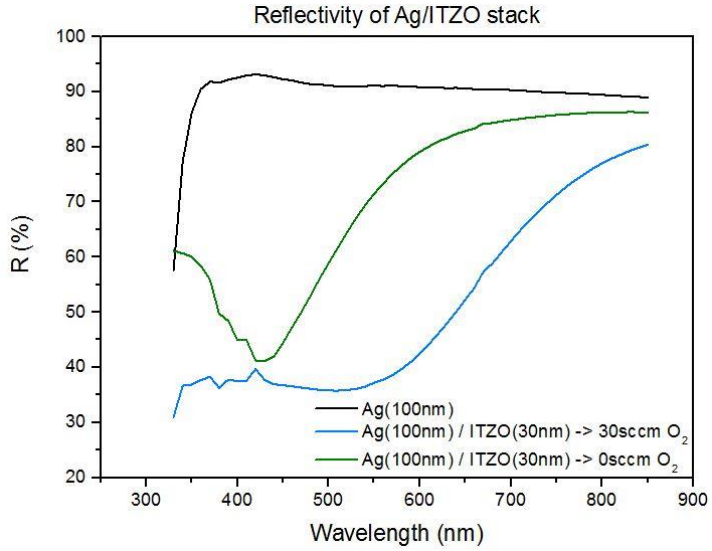

Figure 3.4 - Comparison between a silver single layer reflection and a multilayer structure deposited under different O_2 conditions.

3.2.4 Silver/ITO/ITZO deposition

Indium-tin-oxide (ITO) thin films have been extensively studied for optoelectronics applications because they combine high transmission in the visible and near-IR regions of the electromagnetic spectrum with low electrical resistivity and good carrier injection properties [36].

In this thesis, ITO as an interlayer was investigated as a possible solution to avoid the oxidation process taking place in the sliver cathode. An optical simulation was done to optimize the thicknesses of the individual layers in the multilayer stack, obtaining the highest efficiency OLED. The graphs present in Figure 3.5 illustrate the theoretical results for RGB light outcoupling. A darker shade in the figure means a higher outcoupling constant, so it is possible to observe that the most efficient stack with the

biggest work window is achieved with a layer of 30 nm of ITZO on top of an ITO thin film with a thickness between 75-95 nm.

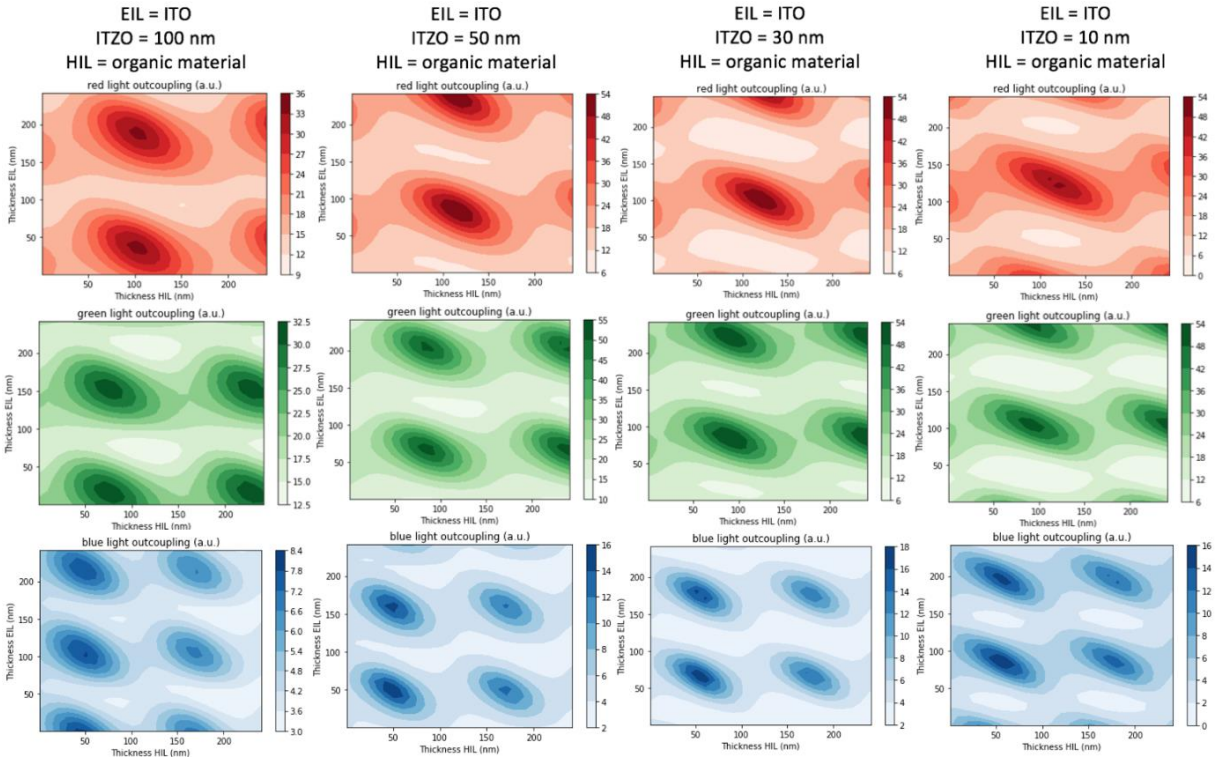

Figure 3.5 – Optical simulation for RGB colors: Y (thickness EIL) and X (thickness HIL) axis represent ITO thickness variation in function of organic material thickness variation, respectively.

Optical simulation only acts as a first indication for the optimal device structure, as it works with a simplified physical model. Thus, a variation of the thickness of the ITO layer was conducted to see the practical effect on the reflectivity of Ag.

The reflectivity spectra of Ag/ITO samples with different ITO thicknesses are shown in Figure 3.6(a). With thicker ITO film, a red-shift of the reflective spectra is observed. The simulation presented in Figure 3.6(b) supports the idea that the shift for long wavelengths could be due to optical effects.

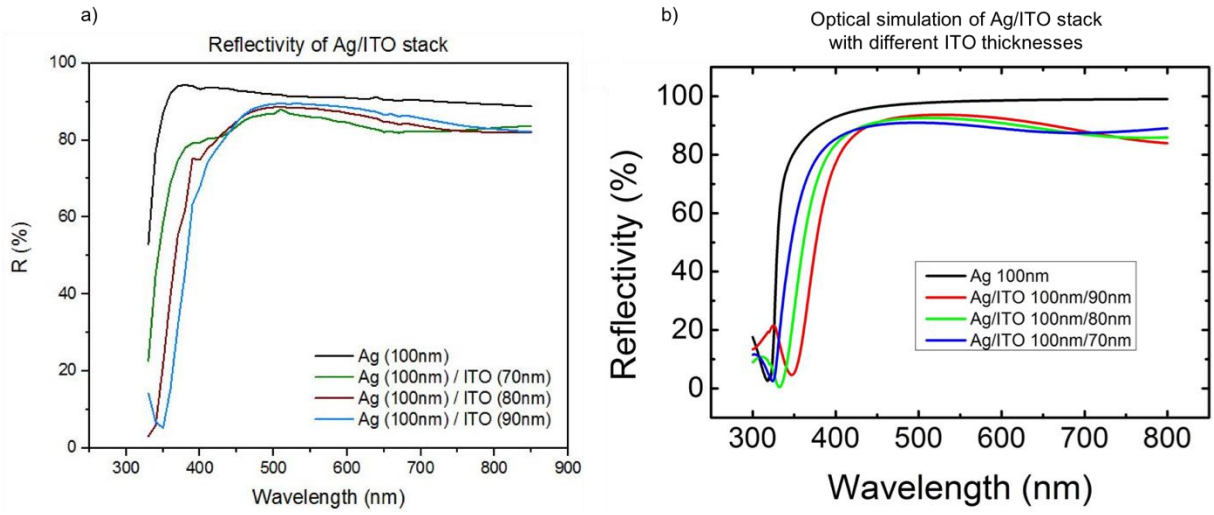

Figure 3.6 – a) Reflective measurements of samples with different ITO thicknesses b) Simulation of samples with different ITO thicknesses.

Finally, an Ag/ITO/ITZO stack was sequentially deposited and optically characterized. Figure 3.7(a) illustrates the wavelength dependence of the reflectivity of that structure. Comparing these results with the results of Figure 3.4, it is possible to see a clear improvement in reflectivity. It could be due to that Ag is protected by ITO from the oxygen during ITZO deposition. Figure 3.7(b) shows the absorption spectra of ITO and ITZO thin films calculated by:

$$T + R + A = 1 \quad (1)$$

where T is transmission, R is reflection and A is absorption. It is possible to comprehend that, for short wavelengths, the low reflectivity is a consequence of high absorption of ITO and ITZO layers.

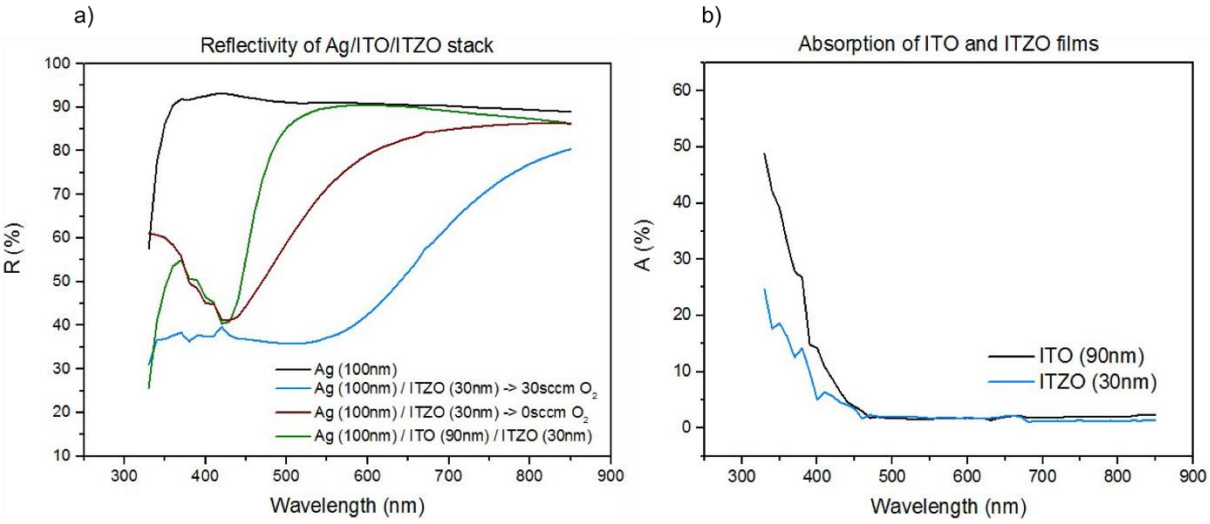

Figure 3.7 – a) Reflectivity of Ag/ITO/ITZO structure b) Absorption of ITO and ITZO films.

As will be presented in section 3.3.2, a difference in etch rate of different materials in the multilayer stack lead to a non-desirable profile after photolithography patterning. Therefore, samples where the thickness of ITO is lower than the thickness of ITZO were also optically investigated. Figure 3.8 depicts the optical simulation results. Another three local maximum were found in optical simulation. One with a structure of ITO(30 nm) / ITZO(~80-90 nm) and other with ITO(10 or 5 nm)/ ITZO (~5 nm).

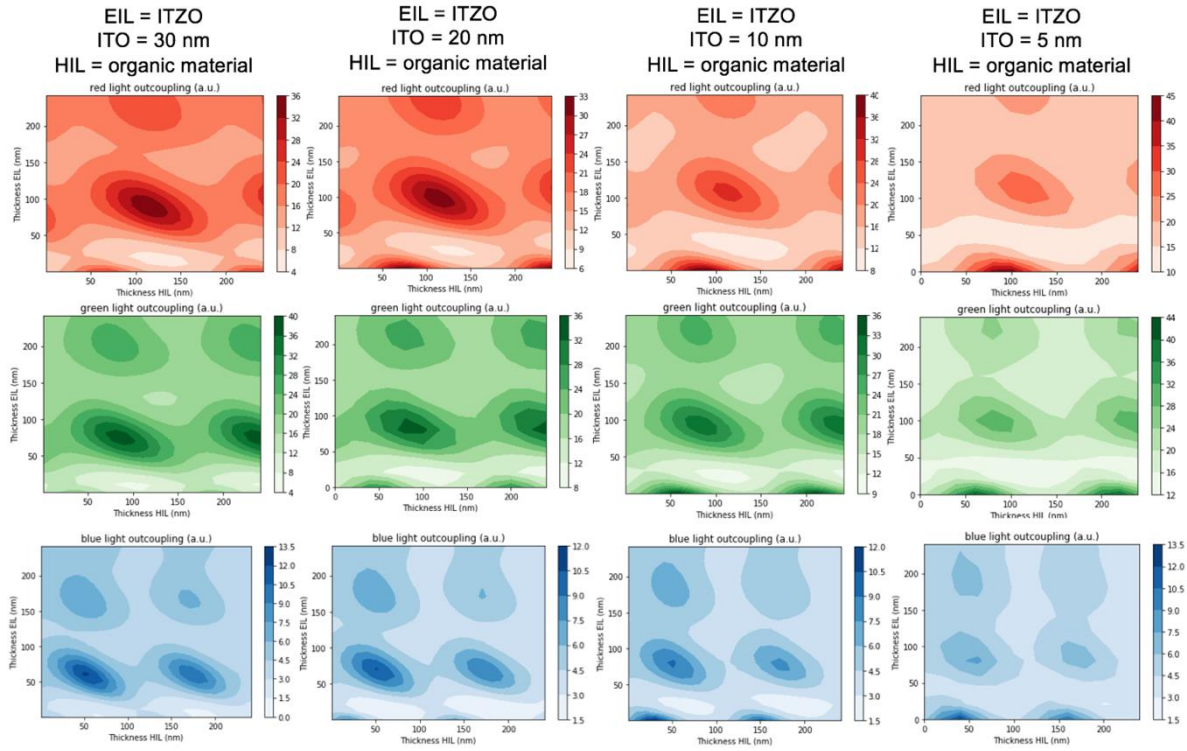

Figure 3.8 - Optical simulation for RGB colors: Y (thickness EIL) and X (thickness HIL) axis represent ITZO thickness variation in function of organic material thickness variation, respectively.

Figure 3.9 illustrates how the thickness of ITO can affect the reflectivity of the Ag(50 nm)/ITO/ITZO(80 nm) structure. The minimum position of the reflectance shifts towards longer wavelengths as the thickness of ITO film increases from 10 to 30 nm, however a similar optical behaviour is reached whether a 10 nm or a 5 nm ITO thickness is employed. This red-shift for higher thicknesses can be a result of optical effects as previous mentioned.

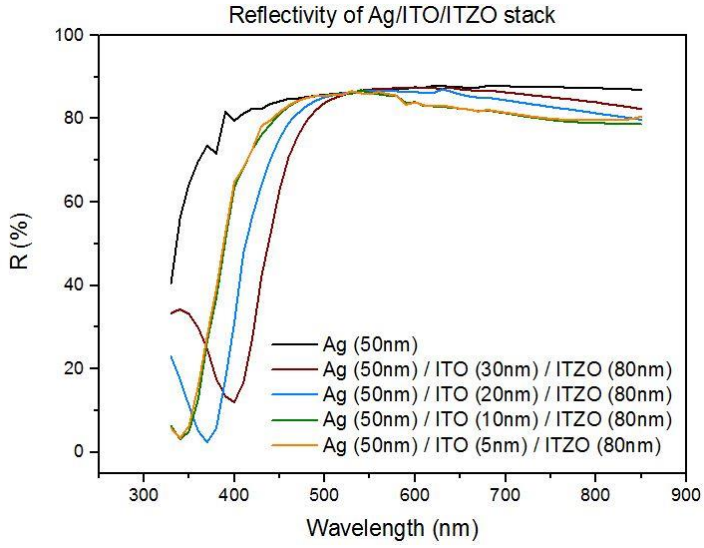

Figure 3.9 - Variation of resistivity with thickness of ITO film on multilayer structure.

Regarding the difficulty in patterning multilayer stack by wet-etching, the effect of a thinner silver layer in the final structure was investigated in Figure 3.10. Almost no difference between the reflectivity of samples using 100nm or 50nm of silver was observed.

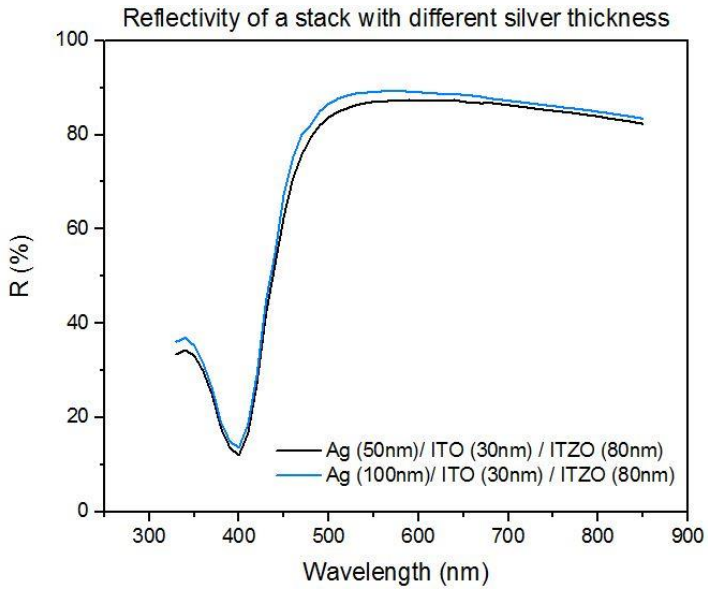

Figure 3.10 – Effect of Ag thickness in the tri-layer structure.

3.3 Photolithography Process: Etching optimization

After optical optimization of the multilayer stack, it was further developed the patterning method for the multilayer stack through a photolithography process using wet etching. In this section, a route to etch the full stack with two etching steps under wet conditions is presented and discussed. A 10% mixed acid etchant solution from Fujifilm is used to etch ITO/ITZO stack together and a 75% phosphoric acid etching mixture from Honeywell is used to etch silver.

3.3.1 Ag (50 nm) etching

To get a rough idea about the etching condition for silver in the final stack wet etching of single silver layer was performed using a 75% PWES solution at 45 °C. Three samples with 50 nm of Ag on top of cleaned glass were immersed in the solution bath during 8,10 and 12 seconds, respectively. AFM images were used to examine the quality of the etching. Table 3.1 shows the profile of a 5μm interdigit of each sample. Structures close to 5 μm with perfect hills and valleys were achieved, although the edge shape and pattern size were not perfect.

Table 3.1 – 50 nm of Silver etching evolution.

8 SEC	10 SEC	12 SEC
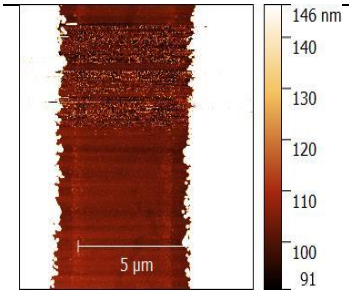	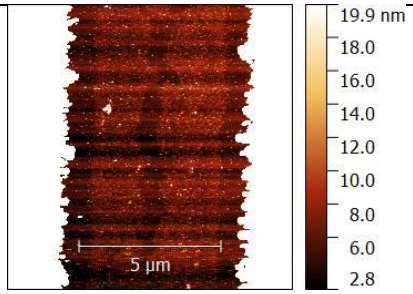	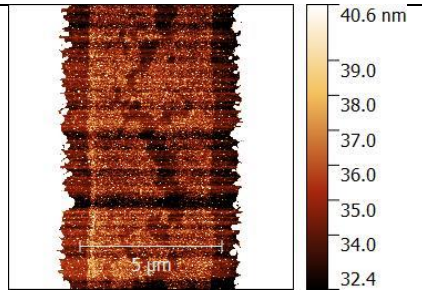

Further optimization is necessary to better understand the previous results, Ag morphologic study after deposition and photoresist line width measurements could have been done.

3.3.2 ITO (90 nm) etching

ITZO wet etching process using 5 % oxalic acid solution at RT has already been optimized with an etch rate of 2.13 nm/sec. To get an impression about the etching conditions for ITO, a sample with 90nm ITO on top of a silicon wafer was exposed to the same etchant and temperature.

Table 3.2 – 90 nm of ITO etching using 5% Oxalic Acid.

6 MIN	10 MIN	18 MIN
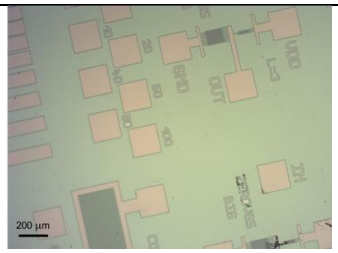	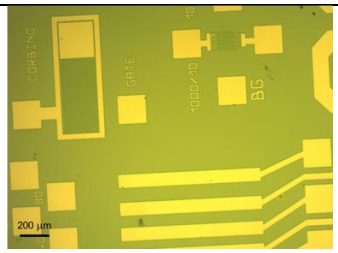	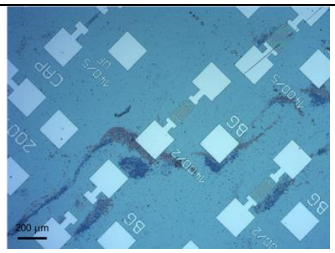

The results of Table 3.2 show the sample appearance after being immersed in 5% oxalic solution during 6, 10 and 18 min. After 18 min, it was still not possible to clearly observe the blue colour of the wafer in the exposed areas, leading to the hypothesis that some ITO on top of the wafer was left over. These results reveal an undesirable difference between the etch rate of both materials using this etchant. In fact, wet etching is an isotropic process, meaning that the etching rate is the same in both horizontal and vertical direction. Consequently, for any dimension to be etched vertical, the etching will also proceed laterally under the resist [41]. Thereby, a double layer sample made of these two materials could not have the desirable shape at the end of the process. Hence, a reduction of ITO thickness in the final stack was studied in section 3.2.4. Because even with thinner ITO thickness, the etch rate would still be very low compared with ITZO, also a new etchant was tested in section 3.3.4 .

3.3.3 ITZO (80 nm) etching

80 nm of sputtered ITZO was patterned using a photolithography process with IX845 photoresist. The etching was done by dipping the sample in a 10% mixed acid etchant solution composed of nitric acid, acetic acid and hydrofluoric acid during 30 sec at RT. AFM images, present in Figure 3.11 , show the profile of a 5 μm interdigit after the process and confirm a film thickness of 80nm. On the other hand, a triangular instead of a rectangular structure is revealed. Besides the strong isotropic effect of a wet etching process, another reasonable explanation for this outcome is the poor adhesion between the photoresist and the ITZO film triggering lateral etching under the photoresist mask [41].

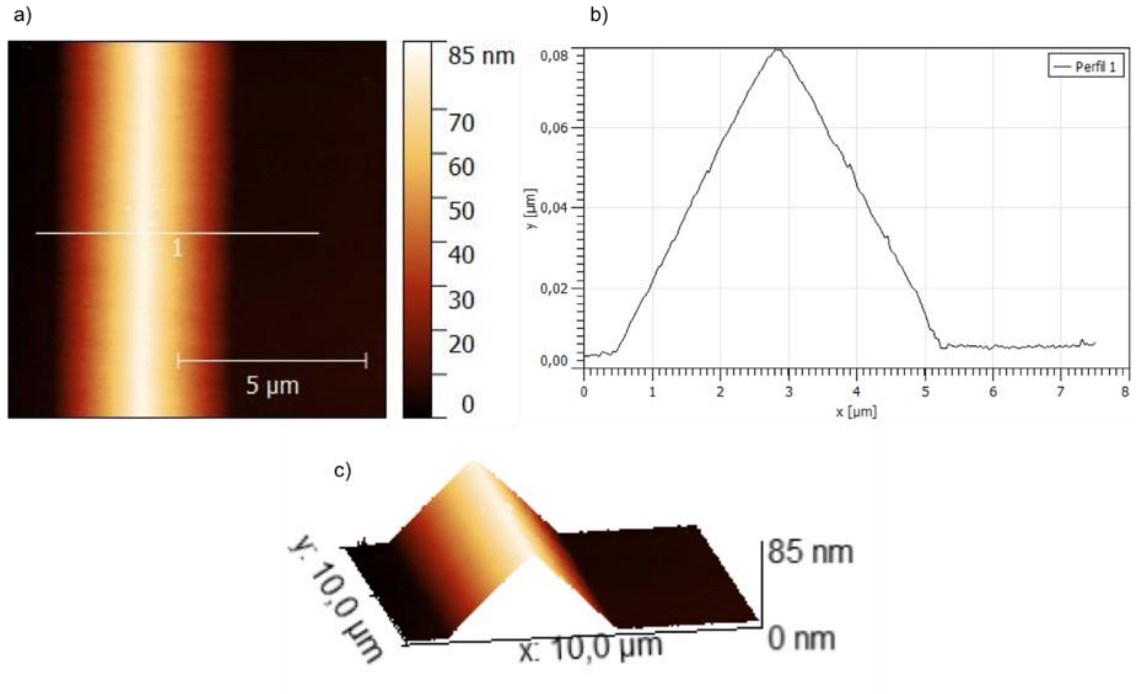

Figure 3.11 - Analyses by AFM of a 5µm interdigit from 80 nm ITZO film patterning without Ti Prime a) height analyses b) profile c) 3D image.

The application of a Ti Prime layer, a highly dilute organic titanium compound, was tested as a solution to improve the photoresist adhesion and avoiding lateral etching [42]. Ti prime was spin-coated on top of ITZO film. Then the adhesion promoter was activated in a subsequent baking step at 120 °C for 1 minute, followed by the immediate application of the photoresist after cooling of the substrate to room temperature. Figure 3.12 shows the atomic force microscope images of a 5 µm interdigit. According to these images, it is possible to conclude that with the application of Ti Prime, the photoresist adhesion was improved and perfect 80nm structures with vertical side walls and well-defined hills and valleys can be achieved.

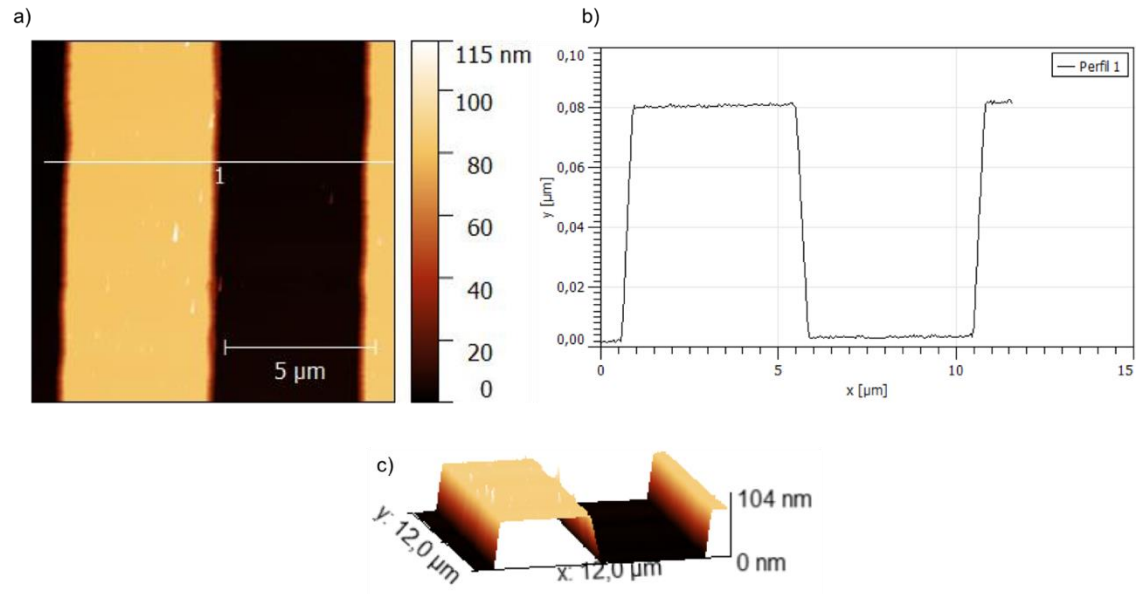

Figure 3.12 - Analyses by AFM of a 5µm interdigit from 80 nm ITZO film patterning with Ti Prime a) height analyses b) profile c) 3D image.

Figure 3.13 displays the well-defined pattern of the same interdigit structure. The yellow pattern is the ITZO film while the brown part represents the silicon wafer. The rounded corners of the openings can be an effect of the isotropic process.

Figure 3.13 – Optical microscope image of a 5μm interdigit from 80nm ITZO film after photolithography process using Ti Prime.

These results confirm that ITZO thin films with 5μm structures can be successfully patterned using 10% mixed acid solution as etchant and Ti Prime as adhesion layer with an etching rate of 2.67 nm/sec.

3.3.4 ITO (5 nm) / ITZO (80 nm) etching

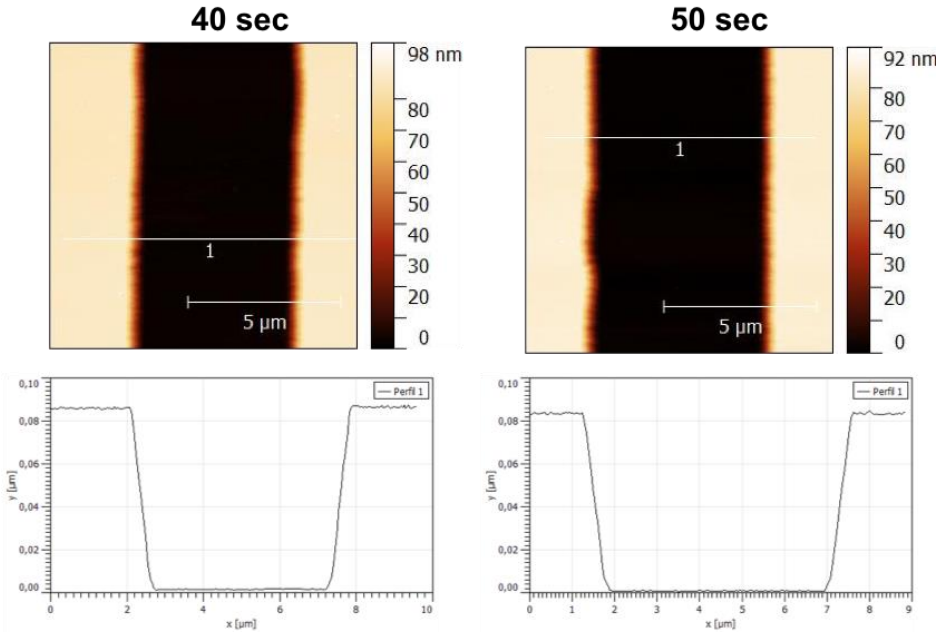

Figure 3.14 – AFM images of samples with a configuration of ITO (5nm) / ITZO (80nm) etching during 40 and 50sec, respectively.

Because 5 nm of ITO is too thin to be observed by microscope, samples with 5 nm of ITO under 80 nm of ITZO were patterned using 10% mixed acid etchant at RT. Different times were tested to optimize the etching process for this double layer structure. Figure 3.14 shows the difference between samples with 40 and 50 sec of etching time. Increasing time leads to an increase of channel length from ~4.4 μm

to 5 μm. As a 5 μm interdigit was being analysed, it is possible to conclude that 50 sec might be the ideal time to etch an 85 nm structure. Once again, perfect hills and valleys were achieved under the previous photolithography conditions.

Figure 3.15 presents the optical image of both samples, where the yellow colour denotes ITO/ITZO stack and the brown part represents the wafer underneath. Observing Figure 3.15(a) it is possible to visualize some thin films residuals, visible by the light blue areas, indicating under-etching in those areas. At the same time, Figure 3.15(b) shows a well-defined 5 μm interdigit without any thin film residuals outside the pattern. It is possible to conclude that 50 sec is the ideal time to etching 85 nm structure on top of a silicon substrate.

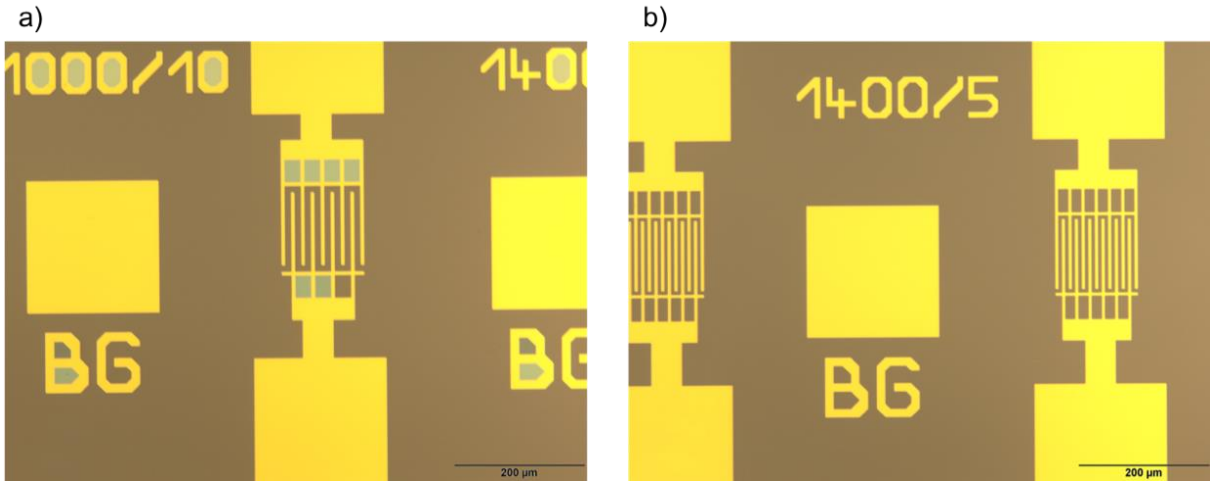

Figure 3.15 -Optical Microscope images of samples with a configuration of ITO (5 nm) / ITZO (80 nm) etching during a) 40 sec and b) 50 sec.

3.3.5 Silver (50 nm) / ITO (5 nm) / ITZO (80 nm) etching

To pattern the full stack, two subsequent wet-etching steps were used during the photolithography process. First, the sample was immersed in 10% mixed acid etchant at RT to remove ITO/ITZO layers, followed by a rinse with deionised water. Then, the sample was dipped in 75% PWES solution at 45 °C to etch the silver layer, also followed by a rise with deionised water. The result of this two consecutives steps is schematized in Figure 3.16

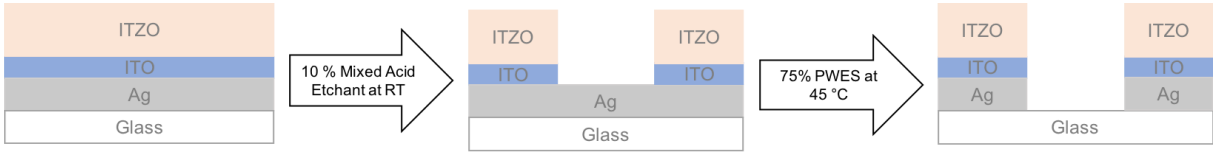

Figure 3.16 – Full stack etching process scheme.

In order to find the proper etch time for Ag and for ITO/ITZO in a full stack structure, a variation in etching time was monitored by AFM and OM images.

Table 3.3 shows the evaluation of the etching depths and the topography aspect versus time when full stack samples were separately dipped in 10% mixed acid etchant. The yellow part of the images is the ITO/ITZO layer and the brown part is silver on top of glass.

Table 3.3 – AFM images of full stack samples dipped in 10% mixed acid etchant for different times.

10 sec	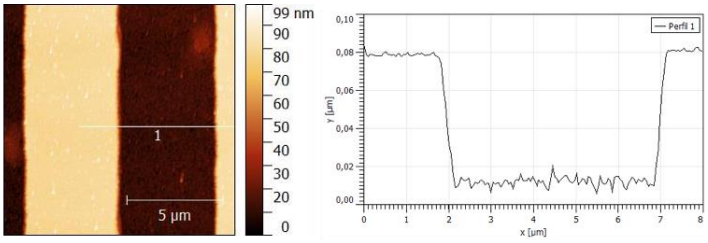
20 sec	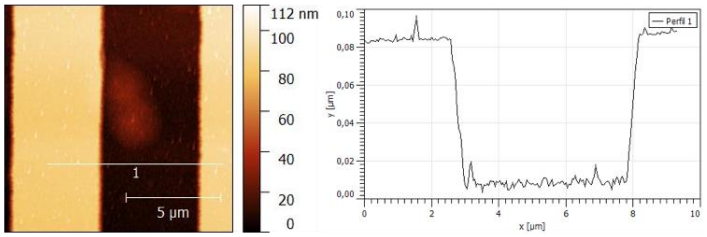
30 sec	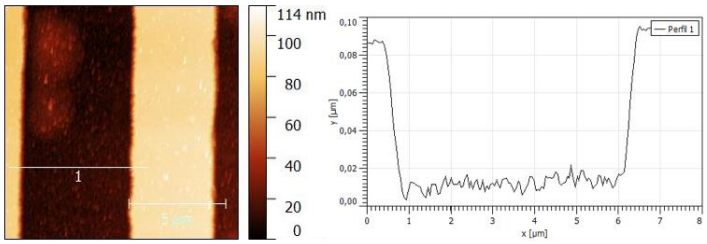
40 sec	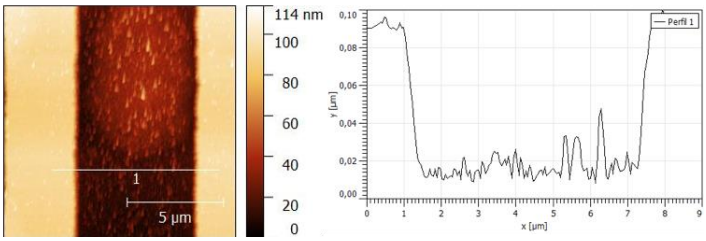

Observing the previous images, it is possible to conclude that increasing the etching time leads to an increase in etch depth. The goal during this step was to etch 85 nm, corresponding to the combined thicknesses of the ITO and ITZO thin films. This was achieved by etching for 30 sec in 10% mixed acid as an etch depth of ~ 84 nm was attained. 40sec etching leads to silver being attacked by the etchant as demonstrate in the shinning zone in the brown part of the image. Looking to the profile, big spikes appeared for 40 sec of immersion, confirming that the silver layer was reacting with the etchant. The roughness of the underlying layer is not crucial in this step as this layer will be later removed. On the other hand, 10 and 20 sec seemed inadequate to etch away the complete ITO/ITZO stack as a depth of ~ 70 and 78 nm, respectively, was reached. At the same time, the channel length of the interdigit was increasing with the time. Because 5 μm interdigit was being analysed, it required 30 sec of etching time to accomplish that feature size.

After removal of the ITO/ITZO layer, the second etch step was carried out inside a 75% PWES solution at 45 °C. Samples were prepared and dipped during 30 sec in 10% mixed acid etchant at RT, then in 75% PWES solution during 4,5 and 6 seconds at 45 °C, sequentially.

Time optimization for this last stage is presented in Table 3.4 samples were prepared and dipped during 30 sec in 10% mixed acid etchant at RT, then in 75% PWES solution during 4,5 and 6 seconds at 45 °C, sequentially.

Table 3.4 and Table 3.5, where AFM images and OM images are presented, respectively. Three samples were prepared and dipped during 30 sec in 10% mixed acid etchant at RT, then in 75% PWES solution during 4,5 and 6 seconds at 45 °C, sequentially.

Table 3.4 - AFM images of full stack samples dipped in 10% mixed acid etchant for 30 sec and then in PWES solution for 4,5 and 6 sec.

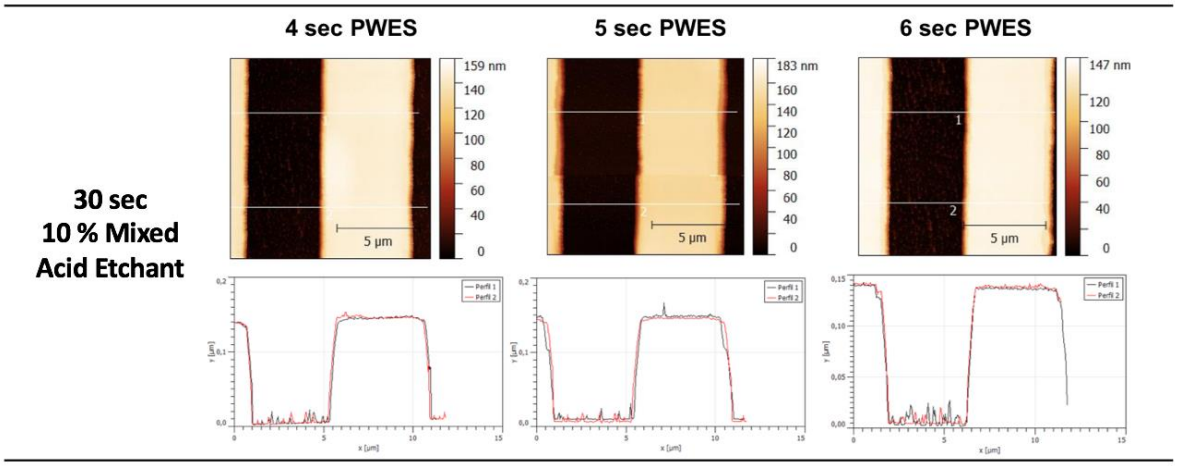

Table 3.5 – Optical microscope images of full stack samples dipped in 10% mixed acid etchant for 20 and 30 sec and then in PWES solution for 4,5 and 6 sec.

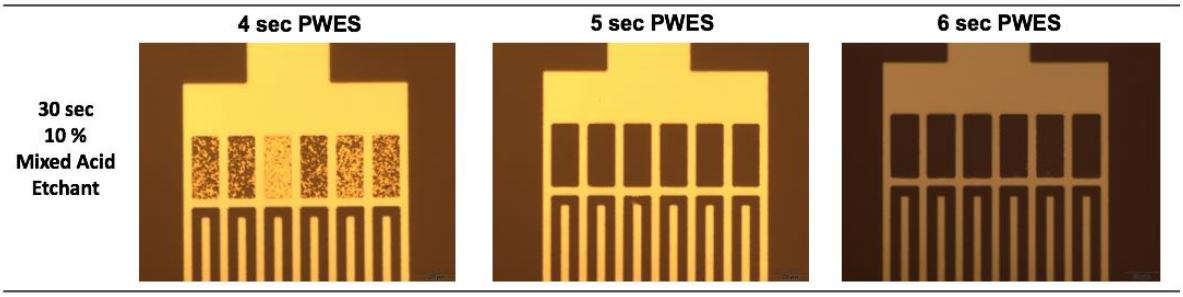

From the previous results it is possible to conclude that to etch away the three layers a combination of 30 sec in 10% mixed acid etchant with at least 5 sec in PWES is necessary. If 4 sec are used, some silver residuals will be present in the bigger openings of the interdigit as can be seen in OM image. For 5 and 6 sec images, no silver residuals remain in the same structures. Thus, 5 sec seems to be enough to etch away all the silver. For an etching time of 6 sec, some small residues are visible in AFM image and the increase in the roughness in that region is confirmed by the AFM profile. This can be due to round to round variation.

At the end, it was possible to confirm that multilayer samples could be successfully patterned with the explained procedure using two wet-etching steps, the first for 30 sec and the second for 5 sec.

4 Summary and Future Perspectives

In top-emission iOLEDs, an extremely reflective cathode and an appropriate electron injection material is required to achieve high luminance efficiency. Among various metals, silver has the highest reflectivity for the visible light [43]. At the same time, ITZO, a transparent amorphous oxide semiconductor, was highlighting as a promising material to decrease the electron injection barrier between the metal cathode and the organic layers [24].

During this dissertation, a highly reflective stack combining the two previous materials was successfully optimized and patterned.

In the first stage of this thesis, it was discovered that thin film silver lost its inherent high reflective properties during ITZO deposition process rather oxygen was introduced in the chamber or not. This can be attributed to silver oxidation induced by the oxygen content present inside the chamber.

Secondly, an ITO interlayer was introduced as a solution to prevent Ag oxidation. While improving the thickness of each film through RT measurements and optical simulation, it was revealed that as ITO gets thinner, the reflectance of the full stack increases across the spectrum due to optical effects. An optimized structure with a configuration of Ag(50 nm)/ITO(5 nm)/ITZO(80 nm) achieved an average reflectivity > 78% in the visible region of the spectrum. It might confirm that an ITO layer acts as a shield, protecting the silver layer from the oxidation process.

Pattern the optimized structure using a wet etching process was the most difficult challenge during this project, because of two reasons. First, the difficulty in finding a suitable etchant for ITO and ITZO together and second the difficulty in reproducing the same results in all the etch trials. At the end, it was concluded that 5% oxalic acid cannot be used to etch ITO and ITZO, as the etch rate of ITO is much lower than the etch rate of ITZO. To overcome this issue, a faster etchant, 10% mixed acid etchant, and a new thickness approach, ITO thinner than ITZO were adopted. It was also settled that, in ITZO thin films, vertical walls can only be achieved when a layer of Ti Prime is spin-coated before coating the sample with photoresist. This is a result of wet etching being an isotropic process, where the etchant chemicals remove substrate material also under the masking material, leading to undesirable etch profiles. Also, the poor adhesion between the photoresist and the material largely contribute for the non-vertical walls.

Although the conductivity of the stack is indeed a decisive factor for its application in OLEDs, due to time constrains, it was not possible to electrically characterize the structure. Hence, further investigations should be done to characterize the electrical potential of this stack.

Moreover, a final top-emission iOLED must be produced to evaluate the applicability of this structure as bottom electrode and electron injection layer. Transfer and Luminance-voltage characteristics should be measured and compared with conventional devices.

References

[1] C. W. Tang and S. A. VanSlyke, “Organic Electroluminescent Diodes,” *Appl. Phys. Lett.*, vol. 51, pp. 913–915, 1987.

[2] G. P. Gonçalves, “Filmes finos de óxido de índio e zinco e sua aplicação em díodos orgânicos emissores de luz,” 2011.

[3] T. Tsujimura, *OLED Display: Fundamentals and Applications*. Wiley, 2012.

[4] H. Fukagawa *et al.*, “Fabrication of 8-inch VGA flexible display using air-stable inverted OLED,” *Dig. Tech. Pap. - SID Int. Symp.*, vol. 45, no. 1, pp. 1561–1564, 2014.

[5] K. Morii *et al.*, “Encapsulation-free hybrid organic-inorganic light-emitting diodes,” *Appl. Phys. Lett.*, vol. 89, no. 18, p. 183510, 2006.

[6] H. Hosono, “Transparent Amorphous Oxide Semiconductors; Materials Design Concept and Device Applications,” *34th Int. Conf. Compd. Semicond. (October 17, 2007, Kyoto)*, vol. 4, no. 2010, pp. 2016–2017, 2007.

[7] H. Fukagawa *et al.*, “Highly efficient and air-stable inverted organic light-emitting diode composed of inert materials,” *Appl. Phys. Express*, vol. 7, no. 8, p. 82104, 2014.

[8] M. P. E. *et al.*, “74-3: Multicolor 1250 ppi OLED Arrays Patterened by Photolithography,” *SID Symp. Dig. Tech. Pap.*, vol. 47, no. 1, pp. 1009–1012.

[9] P. E. Malinowski *et al.*, “Photolithography as enabler of AMOLED displays beyond 1000 ppi,” *Dig. Tech. Pap. - SID Int. Symp.*, vol. 48, no. 1, pp. 623–626, 2017.

[10] H. Hosono, J. Kim, Y. Toda, T. Kamiya, and S. Watanabe, “Transparent amorphous oxide semiconductors for organic electronics: Application to inverted OLEDs,” *Proc. Natl. Acad. Sci.*, vol. 114, no. 2, pp. 233–238, 2017.

[11] T. Schwab, “Top-Emitting OLEDs - Improvement of the Light Extraction of Microcavity Effects for White Emission,” 2014.

[12] S. Hofmann, M. Thomschke, and K. Leo, “Top-emitting organic light-emitting diodes,” vol. 19, no. November, pp. 1143–1147, 2011.

[13] D. Vander Velpen, “Study of efficient and robust high lifetime OLEDs with inclusion of organic and inorganic layers via photolithography processes,” 2017.

[14] C. Qiu, H. Peng, H. Chen, Z. Xie, M. Wong, and H.-S. Kwok, “27.4: Top-emitting Organic Light-Emitting Diode using Nanometer Platinum Layers as Hole Injector,” *SID Symp. Dig. Tech. Pap.*, vol. 34, no. 1, pp. 974–977.

[15] J. N. Bardsley, “International OLED Technology Roadmap,” vol. 10, no. 1, pp. 3–9, 2004.

[16] S. Hofmann, M. Thomschke, P. Freitag, M. Furno, B. Lüssem, and K. Leo, “Top-emitting organic light-emitting diodes: Influence of cavity design,” *Appl. Phys. Lett.*, vol. 97, no. 25, pp. 1–4, 2010.

[17] B. Geffroy, P. le Roy, and C. Prat, “Organic light-emitting diode (OLED) technology: Materials, devices and display technologies,” *Polym. Int.*, vol. 55, no. 6, pp. 572–582, 2006.

[18] P. H. Fukagawa and C. Nhk, “Highly Efficient Inverted OLED with Air-Stable Electron Injection Layer Hirohiko Fukagawa , Katsuyuki Morii *, Yoichi Arimoto *, Mitsuru Nakata , Yoshiki Nakajima , Takahisa Shimizu and Toshihiro Yamamoto,” pp. 1466–1469, 2013.

[19] H. Fukagawa *et al.*, “P-154: Fabrication of 8-Inch VGA Flexible Display Using Air-Stable Inverted

OLED," *SID Symp. Dig. Tech. Pap.*, vol. 45, no. 1, pp. 1561–1564.

[20] H. Hosono, M. Yasukawa, and H. Kawazoe, "Novel oxide amorphous semiconductors: Transparent conducting amorphous oxides," *J. Non. Cryst. Solids*, vol. 203, pp. 334–344, 1996.

[21] J. F. Wager, B. Yeh, R. L. Hoffman, and D. A. Keszler, "An amorphous oxide semiconductor thin-film transistor route to oxide electronics," *Curr. Opin. Solid State Mater. Sci.*, vol. 18, no. 2, pp. 53–61, 2014.

[22] M. Sessolo and H. J. Bolink, "Hybrid organic-inorganic light-emitting diodes," *Adv. Mater.*, vol. 23, no. 16, pp. 1829–1845, 2011.

[23] K. Nomura, H. Ohta, A. Takagi, T. Kamiya, M. Hirano, and H. Hosono, "Room-temperature fabrication of transparent flexible thin-film transistors using amorphous oxide semiconductors," *Nature*, vol. 432, no. 7016, pp. 488–492, 2004.

[24] M. Nakata *et al.*, "Development of flexible displays using back-channel-etched In-Sn-Zn-O thin-film transistors and air-stable inverted organic light-emitting diodes," *J. Soc. Inf. Disp.*, vol. 24, p. n/a-n/a, 2016.

[25] M.-K. Wei, C.-W. Lin, C.-C. Yang, Y.-W. Kiang, J.-H. Lee, and H.-Y. Lin, "Emission Characteristics of Organic Light-Emitting Diodes and Organic Thin-Films with Planar and Corrugated Structures," *Int. J. Mol. Sci.*, vol. 11, no. 4, pp. 1527–1545, Apr. 2010.

[26] H. Cheng, C. Jong, C. Lee, and T. Chin, "Wet-etching characteristics of Ge/sub 2/Sb/sub 2/Te/sub 5/ thin films for phase-change memory," *IEEE Trans. Magn.*, vol. 41, no. 2, pp. 1031–1033, 2005.

[27] S. Mun Lee, B. Hye Choi, J. Soung Park, T. Hoon Kim, H. Kwon Bae, and L. Soon Park, "Effect of ITO/Ag/ITO Multilayer Electrode Deposited onto Glass and PET Substrate on the Performance of Organic Light-Emitting Diodes," *Mol. Cryst. Liq. Cryst.*, vol. 530, pp. 266–271, 2010.

[28] N. Ren, J. Zhu, and S. Ban, "Highly transparent conductive ITO/Ag/ITO trilayer films deposited by RF sputtering at room temperature," *AIP Adv.*, vol. 7, no. 5, p. 55009, 2017.

[29] C. W. Chen, P. Y. Hsieh, H. H. Chiang, C. L. Lin, H. M. Wu, and C. C. Wu, "Top-emitting organic light-emitting devices using surface-modified Ag anode," *Appl. Phys. Lett.*, vol. 83, no. 25, pp. 5127–5129, 2003.

[30] J. Mashaiekhy, Z. Shafieizadeh, and H. Nahidi, "Effect of substrate temperature and film thickness on the characteristics of silver thin films deposited by DC magnetron sputtering," *Eur. Phys. J. Appl. Phys.*, vol. 60, no. 2, p. 20301, 2012.

[31] R. Upadhyay, S. Steudel, M.-P. Hung, A. K. Mandal, F. Catthoor, and M. Nag, "Self-Aligned Amorphous Indium-Tin-Zinc-Oxide Thin Film Transistors on Polyimide Foil," *ECS J. Solid State Sci. Technol.*, vol. 7, no. 4, pp. P185–P191, 2018.

[32] Y. D. Ko and Y. S. Kim, "Room temperature deposition of IZTO transparent anode films for organic light-emitting diodes," *Mater. Res. Bull.*, vol. 47, no. 10, pp. 2800–2803, 2012.

[33] Y. S. Kim, W. J. Hwang, K. T. Eun, and S. H. Choa, "Mechanical reliability of transparent conducting IZTO film electrodes for flexible panel displays," *Appl. Surf. Sci.*, vol. 257, no. 18, pp. 8134–8138, 2011.

[34] A. De Rooij, "The Oxydation of Silver by Atomic Oxygen," *ESA J.*, vol. 13, pp. 363–382, 1989.

[35] A. H. Hammad, M. S. Abdel-Wahab, and A. Alshahrie, “Structural and morphological properties of sputtered silver oxide thin films: The effect of thin film thickness,” *Dig. J. Nanomater. Biostructures*, vol. 11, no. 4, pp. 1245–1252, 2016.

[36] H. Kim *et al.*, “Electrical, optical, and structural properties of indium-tin-oxide thin films for organic light-emitting devices,” *J. Appl. Phys.*, vol. 86, no. 11, pp. 6451–6461, 1999.

[37] F. Aiping, “Indium-Tin Oxide: Its Preparation, Properties and Characterization,” pp. 34–66, 2003.

[38] Z. Ghorannevis, E. Akbarnejad, and M. Ghoranneviss, “Structural and morphological properties of ITO thin films grown by magnetron sputtering,” *J. Theor. Appl. Phys.*, vol. 9, no. 4, pp. 285–290, 2015.

[39] A. Bouzidi, K. Omri, L. El Mir, and H. Guermazi, “Preparation, structural and optical investigations of ITO nanopowder and ITO/epoxy nanocomposites,” *Mater. Sci. Semicond. Process.*, vol. 39, pp. 536–543, 2015.

[40] F. H. Alsultany, N. M. Ahmed, and M. Z. Matjafri, “Effect of varying film thickness on the properties of indium tin oxide films after temperature annealing,” *Int. J. Enhanc. Res. Sci. Technol. Eng.*, vol. 3, no. 6, pp. 443–446, 2014.

[41] “WET CHEMICAL ETCHING - BASICS.” [Online]. Available: https://www.microchemicals.com/technical_information/wet_etching.pdf. [Accessed: 06-Sep-2018].

[42] “Basics of microstructuring - substrate preparation.” [Online]. Available: https://www.microchemicals.com/downloads/application_notes.html. [Accessed: 06-Sep-2018].

[43] J. Cao, X. Jiang, and Z. Zhang, “MoOx modified Ag anode for top-emitting organic light-emitting devices,” *Appl. Phys. Lett.*, vol. 89, no. 25, p. 252108, 2006.

Appendix A

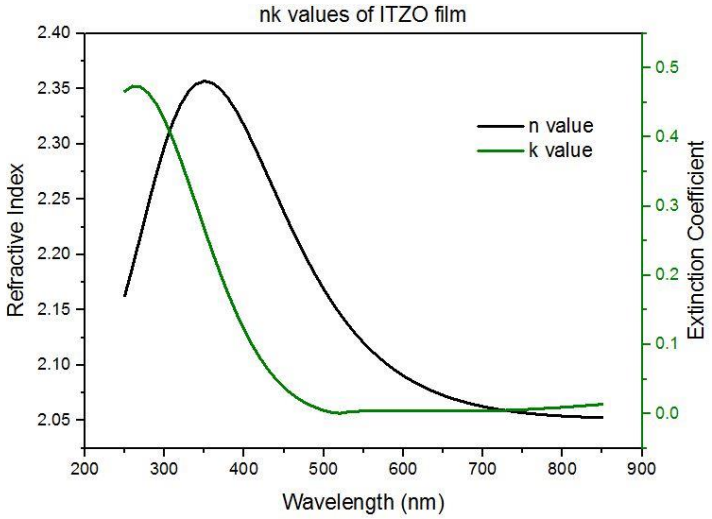

Figure A.1 – nk values of an ITZO thin film deposited by sputtering.

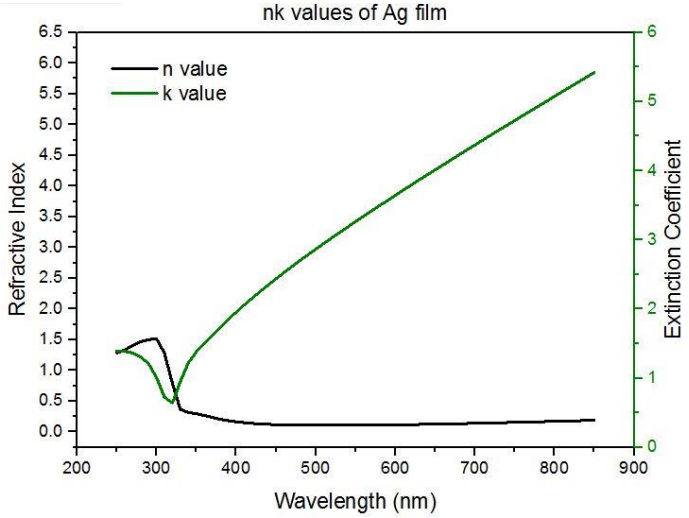

Figure A.2 – nk values of a silver thin film deposited by sputtering.

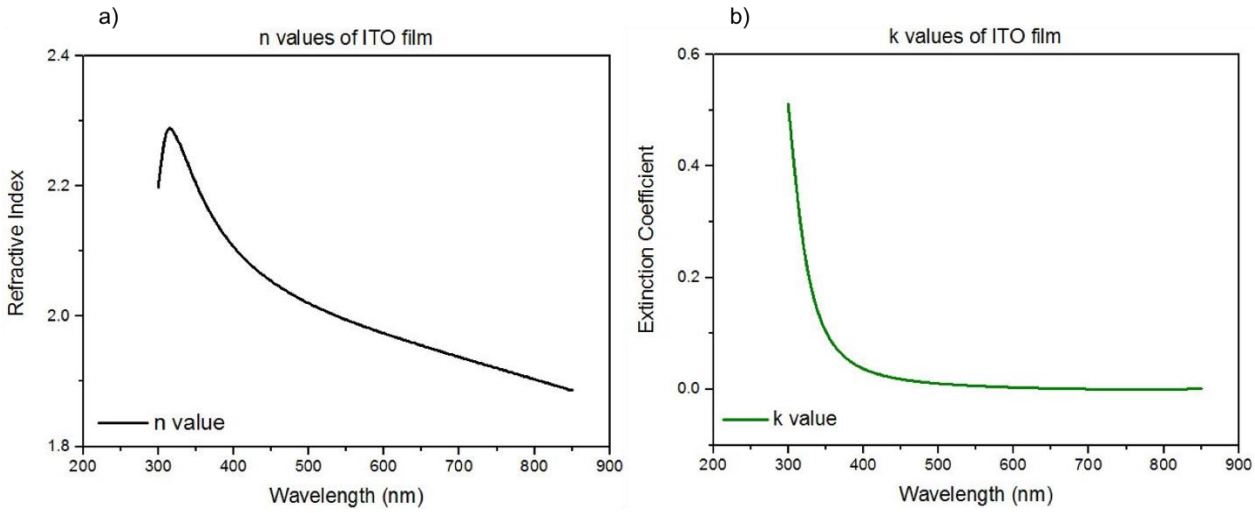

Figure A.3 - a) n value and b) k value of an ITO thin film deposited by sputtering.